Journal of Power Sources 210 (2012) 110–115

Contents lists available at SciVerse ScienceDirect

Journal of Power Sources

journal homepage: www.elsevier.com/locate/jpowsour

# Electrochemical properties of $Li_2O$–$2B_2O_3$ glass-modified $LiMn_2O_4$ powders prepared by spray pyrolysis process

Seung Ho Choi, Jung Hyun Kim, You Na Ko, Young Jun Hong, Yun Chan Kang*

*Department of Chemical Engineering, Konkuk University, 1 Hwayang-dong, Gwangjin-gu, Seoul 143-701, Republic of Korea*

ARTICLE INFO

*Article history:*
Received 7 January 2012
Received in revised form 7 March 2012
Accepted 10 March 2012
Available online 21 March 2012

*Keywords:*
Cathode material
Spray pyrolysis
Lithium manganate
Glass material

ABSTRACT

$Li_2O$–$2B_2O_3$ glass-modified $LiMn_2O_4$ cathode powders are prepared using spray pyrolysis. The powders with 1 and 5 wt% glass material have a spherical shape, dense structure, and large grain size. The BET surface areas of $LiMn_2O_4$ powders with 0 and 1 wt% glass material are 15.0 and 5.9 $m^2\,g^{-1}$, and their mean crystallite sizes are 29 and 49 nm. The lithium boron oxide (LBO) glass material improves the cycle properties as well as the initial discharge capacities of the $LiMn_2O_4$ powders at a constant current density of 1 C. The discharge capacity of $LiMn_2O_4$ powders without any glass material decreases from 116.3 to 92.6 mAh $g^{-1}$ after 100 cycles, the reduced capacity being 80% of the initial capacity. However, the discharge capacity of the $LiMn_2O_4$ powders with 1 wt% glass material decreases from 131.0 to 113.2 mAh $g^{-1}$ after 100 cycles; thus, the capacity retention is 86% of the initial capacity.



## 1. Introduction

Currently, extensive studies are being carried out on the feasibility of using $LiMn_2O_4$ as a substitute for $LiCoO_2$. This is because $LiMn_2O_4$ is more advantageous than $LiCoO_2$ in terms of cost-effectiveness and environment friendliness [1–5]. However, a $LiMn_2O_4$ electrode suffers a severe capacity fading problem after long-term cycling, induced by the dissolution of the electrode into the electrolyte (as $Mn^{2+}$) and a phase transition due to the Jahn–Teller distortion, and such a problem limits its practical application [6]. Many studies have focused on improving the cycling behavior of $LiMn_2O_4$. Among the different routes, surface modification by stable oxide materials has proved to be effective [7–11].

A lithium boron oxide (LBO) glass material has also been used as a coating material because of its high lithium ionic conductivity, good wetting properties, and relatively low viscosity [12–15]. Electrochemical studies have shown that these materials are stable against high oxidation potentials of 4 V cathode electrode materials used in Li-ion batteries today [12]. In the previous reports, glass-coated $LiMn_2O_4$ powders were prepared by a two-step process. The prepared $LiMn_2O_4$ powders are coated with an LBO glass material via solid-state and sol-gel methods [13,14]. A one-step process for the preparation of surface-modified cathode powders would be advantageous in respect of the production cost.

Spray pyrolysis, which is a gas-phase reaction method, is advantageous for the preparation of fine cathode powders with a spherical morphology [16–23]. However, direct surface modification of cathode powders with an oxide material has rarely been performed using spray pyrolysis. In this study, LBO-glass-modified $LiMn_2O_4$ cathode powders were prepared by spray pyrolysis. Modification with the LBO glass material improved the electrochemical properties as well as morphological characteristics of the powders.

## 2. Experimental

A schematic diagram of the ultrasonic spray pyrolysis system used in this study has been presented in a previous paper [24]. The equipment consisted of six ultrasonic spray generators operating at 1.7 MHz, a tubular quartz reactor, and a bag filter. The length and diameter of the quartz reactor were 1200 and 50 mm, respectively. The reactor temperature was maintained at 900 °C. The flow rate of the air used as the carrier gas was 10 L $min^{-1}$. An aqueous spray solution was prepared by dissolving lithium nitrate ($LiNO_3$, Junsei) and manganese nitrate hexahydrate [$Mn(NO_3)_2{\cdot}6H_2O$, Junsei] in distilled water. The amount of lithium added to the spray solution was in excess of 5 wt% of the stoichiometric amount to facilitate the formation of $LiMn_2O_4$ powders. For $Li_2O$–$2B_2O_3$ glass coating material, lithium nitrate ($LiNO_3$, Junsei) and boric acid ($H_3BO_3$, Aldrich) were dissolved into the above spray solution of Li and Mn components. The precursor particles obtained by ultrasonic spray pyrolysis were post-treated at a temperature of 650 °C for 3 h in an air atmosphere.

The crystal structures of the prepared cathode powders were investigated using X-ray diffractometry (XRD; RIGAKU DMAX-33) with Cu Kα radiation (λ = 1.5418 Å). The morphological characteristics of the powders were investigated using scanning electron

* Corresponding author. Tel.: +82 2 2049 6010; fax: +82 2 458 3504.
*E-mail address:* yckang@konkuk.ac.kr (Y.C. Kang).

0378-7753/$ – see front matter © 2012 Elsevier B.V. All rights reserved.
doi:10.1016/j.jpowsour.2012.03.016

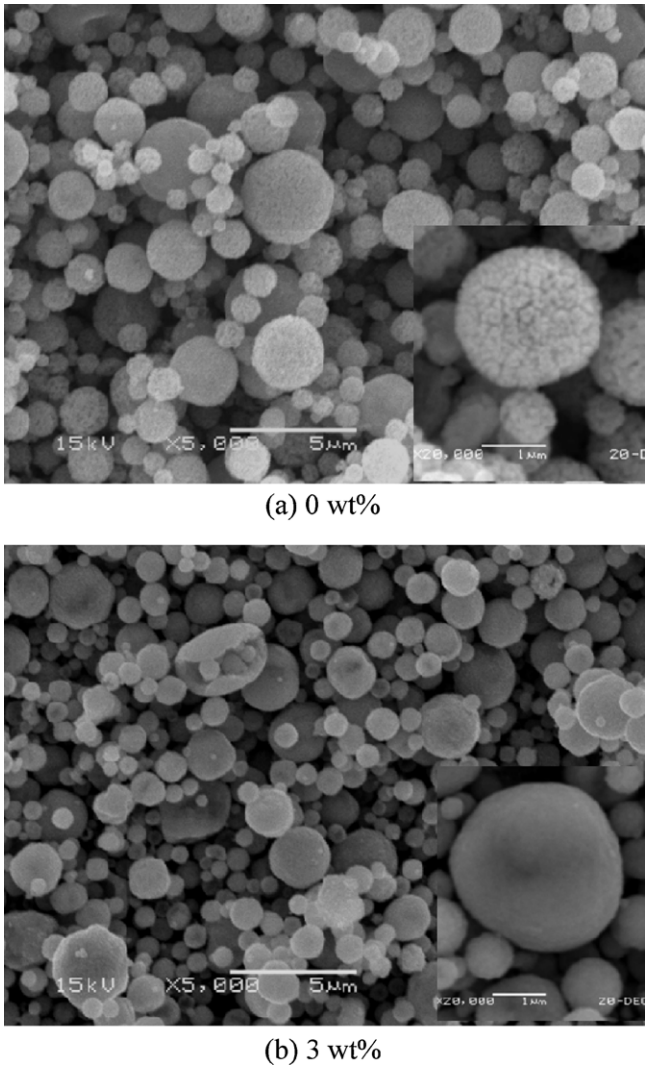


**Fig. 1.** SEM images of the precursor powders with and without glass material: (a) 0 wt% and (b) 3 wt%.

microscopy (SEM; JEOL JSM-6060). The capacities and cycle properties of the powders were determined by using a 2032-type coin cell. The cathode electrode was prepared from a mixture containing 20 mg of $LiMn_2O_4$ and 12 mg of TAB (TAB is a mixture of 9.6 mg of teflonized acetylene black and 2.4 mg of a binder). Lithium metal and microporous polypropylene film were used as the anode electrode and separator, respectively. The electrolyte was 1 M $LiPF_6$ in a 1:1 mixture by volume of EC/DMC. The charge/discharge characteristics of the samples were determined through cycling in the 3.2–4.5 V potential range at constant current densities of 1 C (3 mA $cm^{-2}$) and 2 C (6 mA $cm^{-2}$). Cyclic voltammetry measurements were carried out at a scan rate of 0.07 mV $s^{-1}$. Electrochemical impedance spectra of $LiMn_2O_4$ powders without any LBO glass material and with 1 wt% LBO glass material in the fully charged state (4.5 V) were analyzed.

## 3. Results and discussion

The morphologies of $LiMn_2O_4$ powders without any LBO glass material and with 3 wt% LBO glass material, prepared directly by spray pyrolysis, are shown in Fig. 1. The $LiMn_2O_4$ powders had a spherical shape and micron sizes, irrespective of the presence of the glass material. However, the glass material affected the internal structure of the powders, as shown by the high-magnification SEM images in Fig. 1. The formation of a glass material with a low melting point in the powders during the spray pyrolysis process led to the partially melting of the intermediate product to form powders with a smooth surface. On the other hand, the powders without the glass material had a porous structure with large pores.

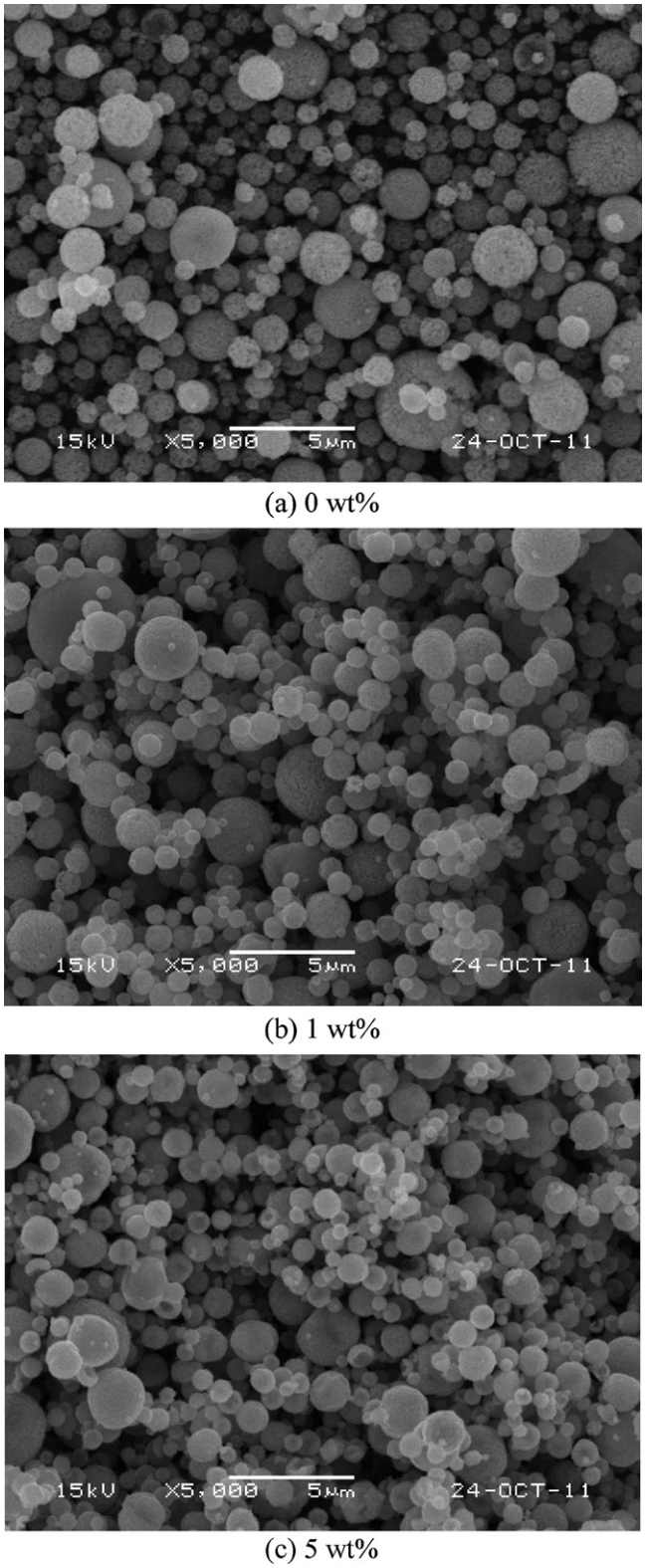


**Fig. 2.** SEM images of the post-treated cathode powders with different glass content: (a) 0 wt%, (b) 1 wt% and (c) 5 wt%.

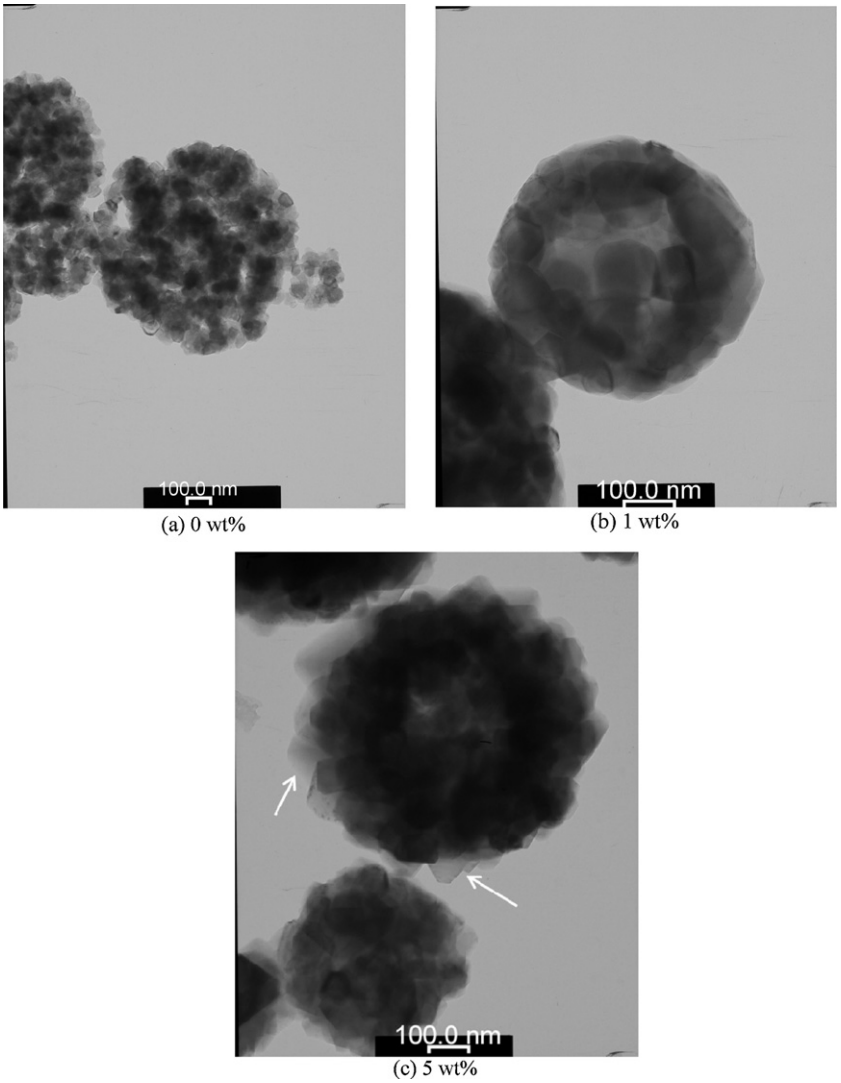


**Fig. 3.** TEM images of the post-treated cathode powders with different glass content: (a) 0 wt%, (b) 1 wt% and (c) 5 wt% (arrows show the facetted crystal structure).

The $LiMn_2O_4$ powders prepared directly by spray pyrolysis had low crystallinity because of the short residence time (1.8 s) of the powders in the hot wall reactor. Therefore, the powders prepared directly by spray pyrolysis were post-treated at 650 °C for 3 h. Figs. 2 and 3 show SEM and TEM images of post-treated $LiMn_2O_4$ powders with different amounts of the LBO glass material. The spherical shape and non-aggregation characteristics of the precursor powders were retained after the post-treatment. TEM images of the $LiMn_2O_4$ powders without the glass material showed a porous structure and a small grain size. On the other hand, $LiMn_2O_4$ powders with 1 and 5 wt% glass material had dense structures and large grain sizes. The LBO glass material also improved the crystallinity of the powders. The $LiMn_2O_4$ powders with 5 wt% glass material had a facetted crystal structure, which is shown by arrows in Fig. 3(c). The pore size distributions of post-treated $LiMn_2O_4$ powders with various amounts of the LBO glass material were analyzed by the Barrett–Joyner–Halenda (BJH) method. The $LiMn_2O_4$ powders without any glass material had a large volume of mesopores and macropores (2–55 nm). The pore volumes of $LiMn_2O_4$ powders with 0, 1, and 5 wt% glass material were 0.06, 0.03, and 0.01 $cm^3\ g^{-1}$, respectively. The pore volume of the $LiMn_2O_4$ powders decreased with increasing glass content, and the powders with 3 and 5 wt% glass material had a dense structure with a small pore volume. The BET surface areas of $LiMn_2O_4$ powders with 0, 0.5, 1, 3, and 5 wt% glass material were 15.0, 9.0, 5.9, 2.7, and 2.9 $m^2\ g^{-1}$, respectively.

Fig. 4 shows X-ray diffraction (XRD) patterns of post-treated $LiMn_2O_4$ powders with various amounts of the LBO glass material. The powders had pure cubic spinel $LiMn_2O_4$ crystal structures irrespective of the amount of glass material. However, the mean crystallite sizes of the powders, calculated by Scherrer's equation from the half-widths of the XRD peaks, were found to be strongly affected by the amount of glass material. The mean crystallite sizes of the $LiMn_2O_4$ powders with 0, 0.5, 1, 3, and 5 wt% glass materials were 29, 41, 49, 49, and 49 nm, respectively. The use of a small amount of glass material, 0.5 wt% of the powders, abruptly increased the mean crystallite size of the $LiMn_2O_4$ powders. However, the $LiMn_2O_4$ powders with glass material content above 1 wt% had similar mean crystallite sizes. Small amount of LBO glass material, with a low melting temperature, improved crystal growth of the $LiMn_2O_4$ powders by acting as a sintering agent. However, high amount of glass material acted as an impurity phase in crystal growth of the powders.

The lattice constants of the $LiMn_2O_4$ powders changed slightly from 8.2211 to 8.2344 Å, depending on the LBO glass material content. The decrease in the lattice constant of the $LiMn_2O_4$ powders by substituting the small radius boron ion to the manganese site did not occur. Therefore, we can conclude that

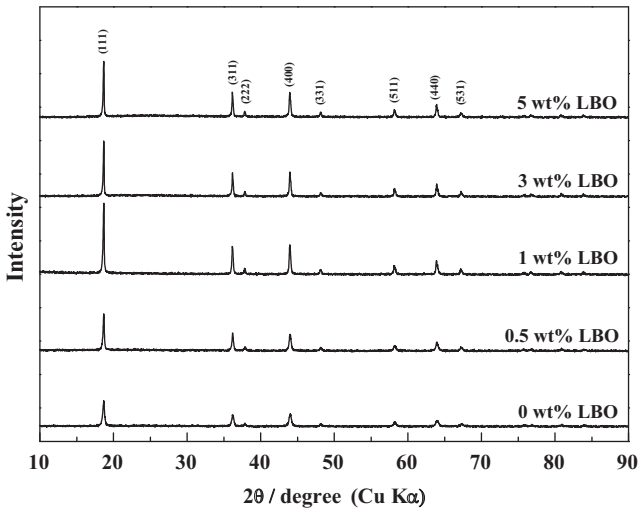


**Fig. 4.** XRD patterns of the post-treated cathode powders with different glass content.

the LBO glass material was formed during spray pyrolysis in the $LiMn_2O_4$ powders. The LBO glass material, with a low melting point, improved crystal growth and promoted the formation of $LiMn_2O_4$ powders with a dense structure.

The effect of the LBO glass content on the initial charge and discharge capacities and cycle properties of the $LiMn_2O_4$ powders was investigated at various current densities. Fig. 5 shows the initial charge and discharge curves of the powders at a constant current density of 1 C for 3.2–4.5 V. The initial discharge capacities of the $LiMn_2O_4$ powders with 0, 1, and 5 wt% glass material were 116, 131, and 124 mAh $g^{-1}$. An appropriate amount of the LBO glass material improved the first charge/discharge capacities and Coulombic efficiencies of the $LiMn_2O_4$ powders. The Coulombic efficiencies of powders without any LBO glass material and with 1 wt% LBO glass material were 94.7 and 97.0%. The optimum amount, 1 wt% of the $LiMn_2O_4$ powders, of glass material improved the initial discharge capacity and Coulombic efficiency of the powders by morphological and structural evolution. 3 wt% glass material is high enough to provide a thoroughly coverage of $LiMn_2O_4$ powders. Therefore, the over-coverage of LBO glass material on $LiMn_2O_4$ powders decreased the initial discharge capacity of 3 and 5 wt% LBO-coated $LiMn_2O_4$ powders.

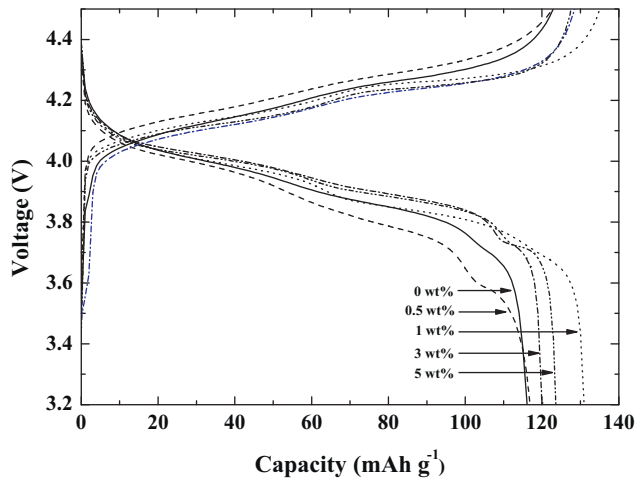


**Fig. 5.** Initial charge and discharge curves of the post-treated cathode powders with different glass content.

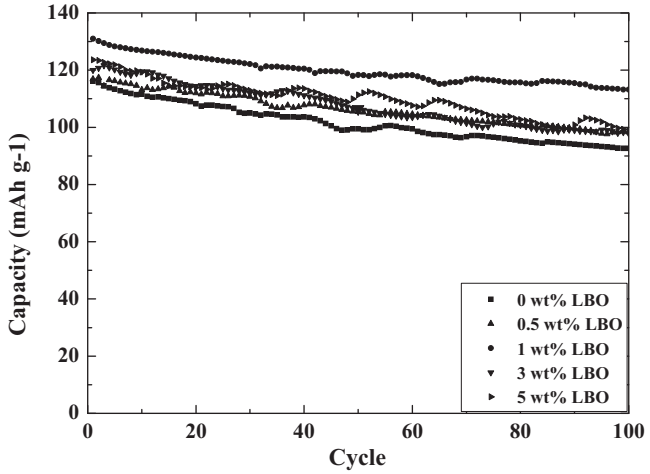


**Fig. 6.** Cycle properties of the post-treated cathode powders with different glass content at room temperature and a constant current density of 1 C.

The cycle properties of the $LiMn_2O_4$ powders with and without the glass material at room temperature are shown in Figs. 6 and 7. The discharge capacities at constant current densities of 1 and 2 C for 3.2–4.5 V are presented in Table 1. The discharge capacity of the $LiMn_2O_4$ powders without any glass material decreased from 116.3 to 92.6 mAh $g^{-1}$ at a constant current density of 1 C after 100 cycles, the capacity retention being 80% of the initial capacity. However, the capacity retention of the $LiMn_2O_4$ powders with 1 wt% LBO glass material was 86% of the initial capacity after 100 cycles. The LBO glass material improved the cycle properties as well as the initial discharge capacities of the $LiMn_2O_4$ powders at a constant current density of 1 C. The optimum amount of LBO glass material was 1 wt% of the $LiMn_2O_4$ powders. The capacity retentions of the $LiMn_2O_4$ powders without any LBO glass material and with 1 wt% LBO glass material were 91% and 98% of their initial capacities after 20 cycles at a constant current density of 2 C. Fig. 8 shows the cycle properties of the $LiMn_2O_4$ powders without and with the LBO glass material at a high temperature of 60 °C. The capacity retentions of the $LiMn_2O_4$ powders with 0, 0.5, 1, 3, and 5 wt% glass material were 84, 86, 88, 92 and 93% of their initial capacities after 50 cycles at a constant current density of 1 C. The high amount of LBO glass coating material improved the cycle properties of the $LiMn_2O_4$ powders at a high temperature 60 °C.

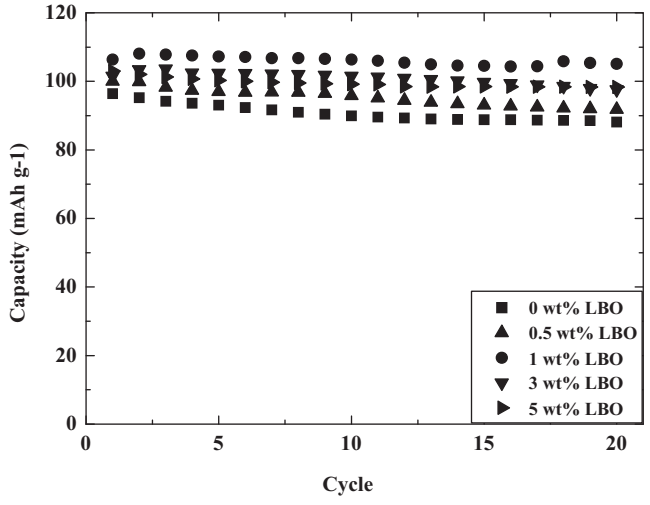


**Fig. 7.** Cycle properties of the post-treated cathode powders with different glass content at room temperature and a constant current density of 2 C.

**Table 1**
Cycling properties of the $LiMn_2O_4$ powders with and without glass materials.

| | 1st (1 C) | 100th (1 C) | Capacity retention (1 C) | 1st (2 C) | 20th (2 C) | Capacity retention (2 C) |
|---|---|---|---|---|---|---|
| 0% LBO | 117 | 93 | 80 | 96 | 88 | 91 |
| 0.5% LBO | 117 | 98 | 84 | 100 | 92 | 92 |
| 1% LBO | 131 | 113 | 86 | 107 | 105 | 98 |
| 3% LBO | 120 | 98 | 82 | 101 | 97 | 96 |
| 5% LBO | 124 | 99 | 80 | 103 | 98 | 95 |

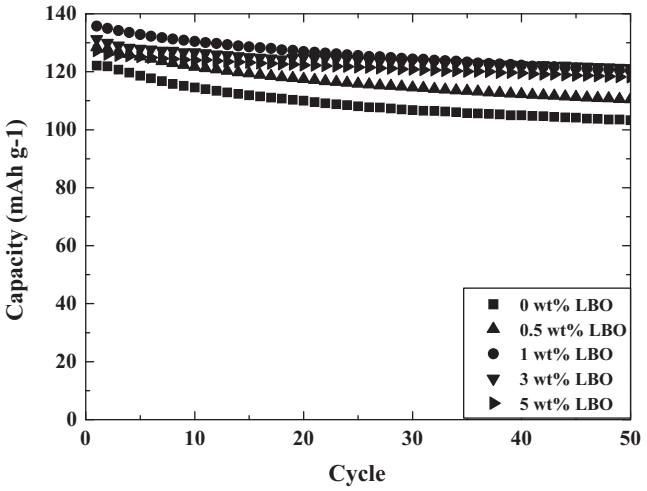


**Fig. 8.** Cycle properties of the post-treated cathode powders with different glass content at 60 °C.

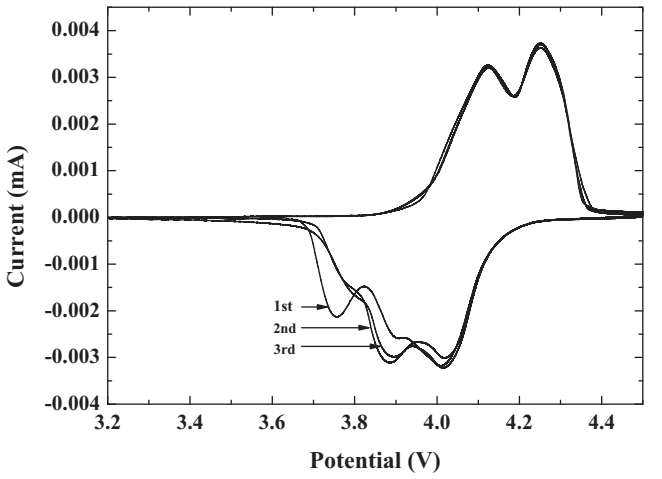


**Fig. 10.** Cycle voltamogram of the post-treated cathode powders with glass material.

Figs. 9 and 10 show cyclic voltammograms of the $LiMn_2O_4$ powders without any LBO glass material and with 1 wt% LBO glass material; the voltammograms were recorded over the voltage range 3.2–4.5 V at a scan rate of 0.07 mV $s^{-1}$. The cyclic voltammogram of the $LiMn_2O_4$ powders without any glass material shows a shift in the oxidation and reduction peaks upon cycling, indicative of a change in the surface structure and composition of the spinel electrode [14]. On the other hand, the cyclic voltammogram of the $LiMn_2O_4$ powders with 1 wt% LBO glass material shows a small peak shift upon cycling. Figs. 11 and 12 show the Nyquist plots of the electrochemical impedance spectra of the $LiMn_2O_4$ powders without any LBO glass material and with 1 wt% LBO glass material in the fully charged state (4.5 V). After 1 cycle, the spectrum of the $LiMn_2O_4$ powders with 1 wt% LBO glass material showed larger impedance than that of the $LiMn_2O_4$ powders without any glass material did. On the other hand, the spectrum of the $LiMn_2O_4$ powders with 1 wt% LBO glass material showed smaller impedance than that of the $LiMn_2O_4$ powders without any glass material did after 50 cycles. The reaction of the $LiMn_2O_4$ powders and electrolyte species generates a highly resistive LiF surface film [25]. However, the LBO glass material covering the $LiMn_2O_4$ powders decreased the amount of resistive material formed on the surface of the active material. The LBO glass material covering the $LiMn_2O_4$ powders improved the electrochemical properties of the powders by decreasing the reactivity of the powders with acidic electrolytes. The high crystallinity of the $LiMn_2O_4$ powders with the glass material also improved the electrochemical properties by increasing the stability of the powders in acidic electrolyte environments.

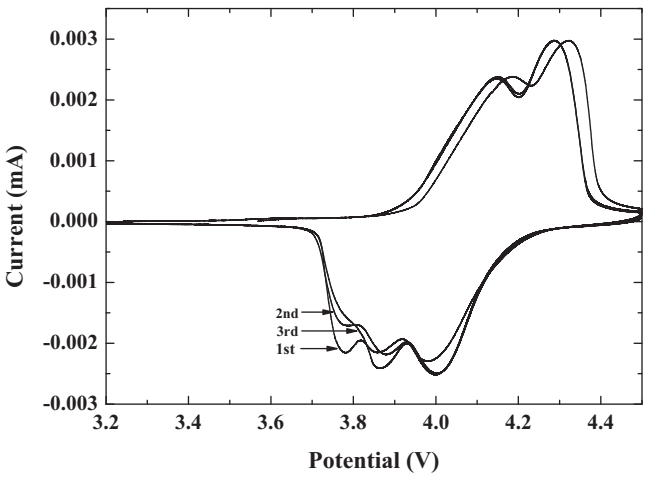


**Fig. 9.** Cycle voltamogram of the post-treated cathode powders without glass material.

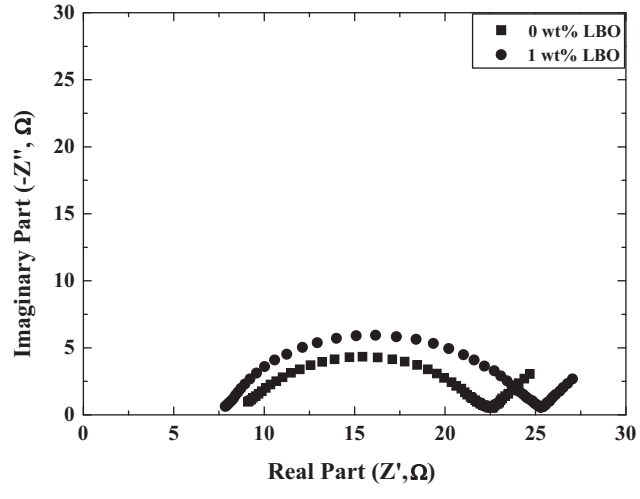


**Fig. 11.** Nyquist plots obtained from the post-treated cathode powders with and without glass material after the 1st cycle.

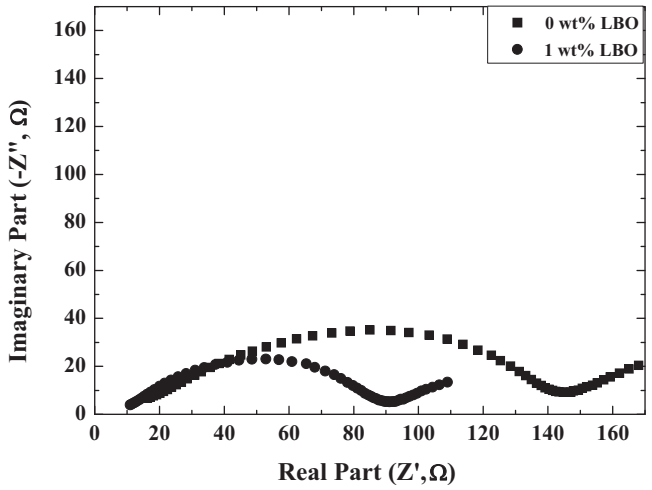


**Fig. 12.** Nyquist plots obtained from the post-treated cathode powders with and without glass material after the 50th cycle.

## 4. Conclusions

LBO-modified $LiMn_2O_4$ cathode powders with a spherical shape, a low surface area, and high crystallinity are prepared by a one-step process using spray pyrolysis. The LBO glass material formed in the $LiMn_2O_4$ powders during the spray pyrolysis process improves the electrochemical properties as well as the morphological characteristics of the powders. The optimum amount of the LBO glass material is 1 wt% of the $LiMn_2O_4$ powder. The addition of an appropriate amount of LBO glass material improves the first charge/discharge capacities, Coulombic efficiencies, and cycle performances of the powders. The LBO glass material covering the $LiMn_2O_4$ powders improves the electrochemical properties of the powders by decreasing the reactivity of the powders with acidic electrolytes.

## References

[1] Y. Xia, Y. Zhou, M. Yoshio, J. Electrochem. Soc. 144 (1997) 115.
[2] J.M. Tarascon, D. Guyomard, Electrochim. Acta 38 (1993) 1221.
[3] T. Ohzuku, M. Kitagawa, T. Hirai, J. Electrochem. Soc. 137 (1990) 769.
[4] J.M. Tarascon, M. Armand, Nature 414 (2001) 359.
[5] D. Guyomard, J.M. Tarascon, J. Electrochem. Soc. 138 (1991) 2864.
[6] T. Aoshima, K. Okahara, C. Kiyohara, K. Shizuka, J. Power Sources 97–98 (2001) 377.
[7] S.W. Lee, K.S. Kim, H.S. Moon, H.J. Kim, B.W. Cho, W.I. Cho, J.B. Ju, J.W. Park, J. Power Sources 126 (2004) 150.
[8] Y.K. Sun, K.J. Hong, J. Prakash, J. Electrochem. Soc. 150 (7) (2003) A970.
[9] S. Guo, X. He, W. Pu, Q. Zeng, C. Jiang, C. Wan, Int. J. Electrochem. Sci. 1 (2006) 189.
[10] Y.K. Sun, K.J. Hong, J. Prakash, K. Amine, Electrochem. Commun. 4 (2002) 344.
[11] M.M. Thackeray, C.S. Johnson, J.S. Kim, Electrochem. Commun. 5 (2003) 752.
[12] G.G. Amatucci, J.M. Tarascon, Solid State Ionics 104 (1997) 13.
[13] H.W. Chan, J.G. Duh, S.R. Sheen, Surf. Coat. Technol. 188 (2004) 116.
[14] H. Şahan, H. Göktepe, S. Patat, A. Ülgen, Solid State Ionics 178 (2008) 1837.
[15] J. Ying, C. Wan, C. Jiang, J. Power Sources 102 (2001) 162.
[16] S.H. Park, C.S. Yoon, S.G. Kang, H.S. Kim, S.I. Moon, Y.K. Sun, Electrochim. Acta 49 (2004) 557.
[17] S.H. Ju, H.C. Jang, Y.C. Kang, Electrochim. Acta 52 (2007) 7286.
[18] I. Taniguchi, C.K. Lim, D. Song, M. Wakihara, Solid State Ionics 146 (2002) 239.
[19] Z. Bakenov, I. Taniguchi, Solid State Ionics 176 (2005) 1027.
[20] Y.N. Ko, H.Y. Koo, J.H. Kim, J.H. Yi, Y.C. Kang, J.H. Lee, J. Power Sources 196 (2011) 6682.
[21] S.H. Ju, Y.C. Kang, Mater. Chem. Phys. 126 (2011) 133.
[22] K. Matsuda, I. Taniguchi, J. Power Sources 132 (2004) 156.
[23] I. Taniguchi, N. Fukuda, M. Konarova, Powder Technol. 181 (2008) 228.
[24] J.R. Sohn, Y.C. Kang, H.D. Park, Jpn. J. Appl. Phys. 41 (2002) 3006.
[25] J.S. Gnanaraj, V.G. Pol, A. Gedanken, D. Aurbach, Electrochem. Commun. 5 (2003) 940.